Hydrol. Earth Syst. Sci. Discuss., https://doi.org/10.5194/hess-2019-204
Manuscript under review for journal Hydrol. Earth Syst. Sci.
Discussion started: 21 May 2019

Hydrology and Earth System Sciences
Discussions

Future shift in winter streamflow modulated by internal variability of climate in southern Ontario

Olivier Champagne[1]*, Altaf Arain[1], Martin Leduc[2], Paulin Coulibaly[1,3], Shawn McKenzie[1]

1 School of Geography and Earth Sciences and McMaster Centre for Climate Change, McMaster University, Hamilton, Ontario, Canada
2 Ouranos and Centre ESCER, Université du Québec á Montréal, Montréal, Québec, Canada
3 Department of Civil Engineering, McMaster University, Hamilton, Ontario, Canada

Corresponding Author: Olivier Champagne, Burke Science Building, Room 313, McMaster University, 1280 Main Street West, Hamilton, Ontario, L8S 4K1, Canada. Email: champago@mcmaster.ca. Tel: (905) 525-9140 ext. 27879

Abstract. Fluvial systems in southern Ontario are regularly affected by widespread early-spring flood events primarily caused by rain-on-snow events. Recent studies have shown an increase in winter floods in this region due to increasing winter temperature and precipitation. Streamflow simulations are associated with uncertainties tied to the internal variability of climate. These uncertainties can be assessed using hydrological models fed by downscaled Global Climate Model Large Ensemble (GCM-LE) data. The Canadian Regional Climate Model Large Ensemble (CRCM5-LE), a dynamically downscaled version of a GCM-LE, was developed to simulate climate variability over northeastern North America under different future climate scenarios. In this study, CRCM5-LE temperature and precipitation projections under RCP 8.5 scenario were used as input in the Precipitation Runoff Modelling System (PRMS) to simulate near future (2040s) streamflow for four watersheds in southern Ontario. Model simulations show that 14% of the ensemble project a high (low) increase of streamflow volume in January-February. Streamflow increases may be driven by rain and snowmelt modulation caused by the development of high (low) pressure anomalies in North America's East Coast. Additionally, the streamflow may be enhanced by high pressure circulation patterns directly over the Great Lakes creating warm conditions and increasing snowmelt and rainfall/snowfall ratio (16%). These results are important to assess the internal variability of the hydrological projections and to inform society of increased winter streamflow.

1 Introduction

Increasing atmospheric greenhouse gases (GHG) concentration is projected to increase air temperatures globally and modify the regional precipitation regimes (Hoegh-Guldberg et al., 2018). GHG-driven climate change is projected to impact watershed fluvial hydrological regimes especially in glaciated or nival catchments (Barnett et al., 2005; Bliss et al., 2014) with serious implications for flood management and water resources (Hamlet and Lettenmaier, 2007; Wu et al., 2015)

The quantification of streamflow and other hydrological processes using hydrological models is becoming an active area of research in various regions of the world. However, the use of hydrological models is subject to a number of choices such as

the Global Climate Model (GCM) and GHG emission scenario (Kour et al., 2016; Stephens et al., 2010), climate data downscaling method (Fowler et al., 2007; Schoof, 2013) hydrological model (Boorman et al., 2007; Devia et al., 2015) and model calibration technique (Khakbaz et al., 2012; Moriasi et al., 2007). In addition, the future temporal evolution of temperature and precipitation patterns will be modulated by the internal variability of climate due to the inherently chaotic characteristic of the atmosphere (Deser et al., 2014; Lorenz, 1963) and will also impact hydrological processes and streamflow (Lafaysse et al., 2014). Therefore, the uncertainties associated with future projections of streamflow and hydrological processes are very high (Clark et al., 2016) and have recently been the subject of intense research (Leng et al., 2016).

The uncertainties due to the internal climate variability is one of the biggest source of uncertainty for the early 21st century hydrological projections (Harding et al., 2012; Hawkins and Sutton, 2009; Lafaysse et al., 2014). The internal variability of climate is a cause of the hiatus observed in global warming in the 2000s (Dai et al., 2015) and is expected to mask the impact of human-induced climate change on precipitation (Rowell, 2012) and streamflow (Zhuan et al., 2018). Single-GCM Large Ensembles (GCM-LE) are based on small initial conditions variations between members of the ensemble and have been used recently to assess the contribution of internal variability on the overall uncertainty of climate-change projections (Deser et al., 2014; Kay et al., 2015; Kumar et al., 2015) and hydrological processes in large watersheds (Gelfan et al., 2015).

Due to GCMs coarse spatial resolution, future climate data should not be used directly for small watersheds hydrological modelling and downscaling techniques must be applied to climate data (Fowler et al., 2007). Statistical downscaling methods are generally preferred as Regional Climate Model Large Ensembles (RCM-LEs) are computationally costly (Lafaysse et al., 2014; Thompson et al., 2015). However, RCM-LEs offer the possibility to relate each member of a Regional Climate Model (RCM) to large scale variability from GCM-LEs. Furthermore, RCM-LEs avoid additional and ambiguous sources of uncertainty from the statistical methods (Gelfan et al., 2015).

The Canadian Regional Climate Model Large Ensemble (CRCM5-LE) is a 50-member regional model ensemble at a 12km resolution produced over northeastern North America in the scope of the Québec-Bavaria international collaboration on climate change (ClimEx project; (Leduc et al., 2019). For the purposes of this study, precipitation and temperature data from CRCM5-LE were used as input in the Precipitation Runoff Modelling System (PRMS), which was applied to four watersheds in southern Ontario. The 50-members were then grouped into classes of similar weather and streamflow projections to assess the impact of internal climate variability on future hydrological processes in southern Ontario. A CRCM5 ensemble was already used as input in multiple hydrological models in a Québec catchment by (Seiller and Anctil, 2014), but this was analyzed for 5 members only. (Erler et al., 2018), used a four-members regional ensemble as input in an integrated surface and groundwater model for the Grand River watershed in southern Ontario. To our knowledge this study is the first time that a 50-members ensemble regional model was used as input in a hydrological model. This analysis, therefore, is very relevant to understand the contribution of anthropogenic and natural forcing on the temporal evolution of runoff in southern Ontario and better predict future streamflow for these watersheds.

This paper is organized as follows: Section 2 presents the PRMS hydrological model, the CRCM5-LE dataset and the classification procedure. Section 3 examines the impact of atmospheric circulation on streamflow projections. Section 4 is dedicated to the discussion of results and the concluding remarks are presented in Section 5.

2 Data and methods

2.1 Study area

Four watersheds in southern Ontario were selected for their long hydrometric time series archives and represent well the diversity of scale, soil type, and land use in this region (Figure 1 and Table 1). Land use in all four watersheds are dominated by agricultural activity. Two major cities, Brantford in Grand River, and London in Thames River are present in the study area and additional urban areas are located in the Credit river watershed. The Big Creek watershed contains the lowest proportion of urbanization (2%). The watersheds also vary in soil type: sand predominates in Big Creek (79%) and Credit River (43%), but a large area of Credit is also covered by loamy soil (49%). Grand River has almost an equal proportion of sand (30%), loam (32%) and clay (38%) while Thames River contains more clay (39%). The elevation is also highly variable with the highest altitudes in the North parts of Grand River (531 m) and Credit River (521 m) watersheds while the lowest areas are located in the sandplains further south in Grand River (178 m) and Big Creek (179 m).

2.2 PRMS hydrological model

The Precipitation Runoff Modelling System (PRMS), a widely used semi-distributed conceptual hydrological model, was applied to all four watersheds. The hydrological calculations in PRMS are based on physical laws and empirical relations between measured and estimated quantities. A series of hydrologic reservoirs are used (plant canopy interception, snowpack, soil zone, subsurface) and the water flowing between the reservoirs are computed for each hydrological response units (HRU). For more information about the structure of this model, refer to (Markstrom et al., 2015).

In this study, HRUs consisted of surface grid cells of 200m² for Big Creek and Credit River watersheds and 400m² for Grand River and Thames River. These latest two watersheds have coarser HRU's to decrease the model time calculation. For each HRU, temperature and precipitation from the closest meteorological measure were used and adjusted according to the altitude and monthly lapse rates calculated for each watershed. The potential evapotranspiration was computed according to the Jensen Haise formulation with air temperature, solar radiation and two additional parameters as inputs: the jh_coef_HRU and the jh_coef. jh_coef_HRU, was estimated for each HRU according to air temperature and elevation and jh_coef, is a coefficient that had to be calibrated. The shortwave solar radiation was estimated by the module ddsolrad, which uses a degree day method. The srunoff_smidx module, a non-linear variable-source area method, was used to compute surface runoff from infiltration and saturation excesses. Routing of flow from upstream to downstream was computing using the Muskingum flow routing method that uses a coefficient (K_coef) to represent stream water travel time in each stream segment. K_coef was estimated for each segment with respect to stream length and stream slope and the coefficient was adjusted during calibration. Parameter

values used by PRMS were found in the literature and were spatialized for each HRU's (Table 2). Arcpy-GSFLOW, a series of ARCGIS scripts creating the HRU's, was used to estimate parameters according to land use, elevation, aspect, slope and soil type. Arcpy-GSFLOW was also used to estimate the water cascade between the HRU's and the river segments. Some of these parameters were modified during calibration to keep the relative spatial variability (Table2).

Five years were used as the initialization period (Oct 1984-Sept 1989) to remove the error due to initial conditions. Different simulations with a varying initialization period length were tested in the Big Creek watershed and showed that five years were necessary for the hydrological model to forget the initial conditions of the reservoirs. The calibration period was between Oct 1989 and Sept 2008 and the years 2009 to 2013 was used as the validation period. The input variables for PRMS are precipitation, minimum temperature and maximum temperature values. These variables were taken from the gridded historical weather station data (CanGRD) produced by (McKenney et al., 2011) using Natural Resources Canada and ECCC data archives at 10 km spatial resolution. 186 data points were needed to cover the area of the four watersheds (red markers on Figure 1). For model calculations, each HRU used climate data from the closest grid point.

The best set of parameters retained after calibration is shown in Table 3. The Nash Sutcliff Efficiency (NSE) values are always higher than 0.65 for both calibration and validation periods (Table 3). The percent bias (PBIAS) is between -15% and +15% except for Credit River during the validation period. A NSE higher than 0.65 and a PBIAS lower than 15% is generally considered a good quantitative fit (Moriasi et al., 2007). Figure 2 shows the simulation and the observation of the daily streamflow in all four watersheds and confirms visually the goodness of simulation fit.

2.3 Climate data projections

The future climate data used as input in PRMS were from the Canadian Regional Climate Model Large Ensemble (CRCM5-LE), a 50-member ensemble of climate change projections at 0.11° (~12-km) resolution. This regional ensemble, computed with the Canadian Regional Climate Model (CRCM5), consists of downscaled data from the 2.8° (~310 km) resolution CanESM2 50-member Large Ensemble (CanESM2-LE). The ensemble extends from the historical (1954-2005) to the forecasted (2006-2099) period forced with the RCP8.5 scenario. The CRCM5-LE Data grid-points the closest to CanGRD data points were used in this study. For each coupled CRCM5-LE/CanGRD grid point, the climate data from CRCM5-LE were bias-corrected over the historical period (1954-2005) using the method developed by (Ines and Hansen, 2006). A gamma distribution was used for both observed and modelled precipitation intensities while a normal distribution was used for the temperature bias correction. These bias-correction calculated from the historical period were then applied to the CRCM5-LE grid points for the entire period 1954-2099.

2.4 Ascending hierarchical classification

An ascending hierarchical classification (AHC) was used to classify all 50 members into classes of similar change of streamflow and meteorological conditions. The AHC was applied to the 4-watersheds January-February normalized change of streamflow and regional change of temperatures/precipitation between the historical (1961-1990) and 2040's periods (2026-

2055). The AHC was performed using January-February data because these months correspond to a large change of streamflow during the period. For precipitation and temperature, the period from 25 December to 22 February was used to account for the delay between weather conditions and stream flow at the outlet. A delay of 6 days showed the best correlation between the increase in temperature and precipitation and the increase of streamflow for all 4 watersheds.

The future projection of atmospheric circulation for each class was analysed using climate variables from CanESM2-LE with a geographical domain from 30°N to 60°N latitude and 100°W to 50°W longitude. Climate variables used for analysis included air temperature at 850hPa level (850T), precipitation (PP), sea level pressure (SLP), geopotential height at 500hPa (Z500) and surface winds. These climate variables were separated into internal and forcing contributors. The forcing contribution of the climate variables corresponded to the average change of all ensemble members between the historical period and 2040s. The internal contribution associated to each member was calculated by subtracting the original member data from the forcing contribution. This method was previously used by (Deser et al., 2014) to assess the internal contribution of future change in temperature and precipitations in North America.

3 Results

3.1 Streamflow projections

Figure 3 shows the average daily streamflow volume and the number of high flows for all members for the historical (Hist) and future (2040s and 2080s) periods. Observational streamflow (OBS) and the controlled streamflow simulated with CanGRD data (CTL) are also shown for the historical period.

In the historical period, average streamflow from the OBS, CTL and the 50-member data sets followed similar annual cycles with the first peak of the hydrological year occurring in November-December and the highest peak in March-April. By 2040 a clear peak in streamflow and the number of high-flow events is still modelled in March but by 2080 the monthly maximum streamflow is more evenly distributed among winter months. This result suggests a progressive shift from two maximal peaks to one winter peak through the 21st Century The simulated range of streamflow volume and number of high flows is high among the 50 different members in winter.

Daily rainfall, snowmelt, and actual ET are also expected to change for the future periods (Figure 4). The amount of rain is simulated to consistently increase among the 50-member average in winter and early spring in all four watersheds. In summer, PRMS simulates future average rainfall to decline, but the direction of change is inconsistent between individual members. The amount of snowmelt is expected to shift from high melt volume in March to a volume consistent throughout the winter. In November and in March-April, snowmelt declines are excepted through the entire 21st century. In January-February, future snowmelt is expected to increase before 2040 followed by snowmelt decreases in all watersheds except Credit River, which shows increases in snowmelt through the later part of the 21st century. Future ET will slightly increase in winter following by dramatic increases in spring period (March and April). In summer ET is simulated to slightly decrease on average but the

difference between the member with the highest and the member with the lowest ET amount is larger as compared to winter ET values.

Figure 5 shows the 50-member future temporal evolution of temperature and precipitation for all four watersheds. Air temperature is shown to consistently increase for all months while the range of precipitation amounts projected by the 50 members is higher. On average, simulated precipitation increases in November-April and decreases in June and September for most of the 21st Century. In July and August, precipitation is simulated to decrease in the near future but to recover by the end of the 21st Century.

3.2 January-February streamflow projections variability

Three streamflow classes and four weather classes were identified based on the minimal interclass Euclidean distance variance among all class number possibilities calculated by the Ascending Hierarchical Classification (AHC) (Figure 6). Three streamflow classes (HiQ, MoQ and LoQ for high, medium and low increase of streamflow) and four weather classes (HiPT, MoPT, LoPT and HiT) were identified. Three weather classes (HiPT, MoPT and LoPT) show a gradient from high to low increase for both precipitation and temperature while one weather class (HiT) show a high increase in temperature only (Figure 6).

The two classes were then aggregated to form a combination of streamflow and weather classes (Table 4). Seven out of the eight members from class HiPT show a large increase of streamflow (HiQHiPT) while one member show a moderate increase (MoQHiPT). Eight of the 13 HiT members show a moderate increase of streamflow (MoQHiT) while four have a low increase (LoQHiT) and one has a high increase (HiQHiT) of streamflow. MoPT has the greatest number of members and consists of eight members that demonstrates low increases of streamflow (LoQMoPT) and eleven members demonstrating moderate increase (MoQMoPT). Lastly, the class LoPT consists of members with the lowest change of precipitation and temperature with three members that show moderate increases of streamflow (MoQLoPT) and eight members showing a low increase (LoQLoPT). The interclass variability is generally consistent between watersheds with the exception of Big Creek. In Big Creek the classes HiQHiT and LoQHiT show relatively low streamflow increases as compared to the other three watersheds (Table 4).

Figure 7 shows scatter plots of averaged change of streamflow to average change of precipitation, temperature, snowmelt and rain between the historical period and simulated values for the 2040s period for all nine classes shown in Table 4. HiQHiPT and LoQLoPT classes are associated with the highest (lowest) increases of streamflow due to high (low) increases of snowmelt and rain (Figure 7). MoQLoPT also demonstrates a larger increase in simulated streamflow compared to LoQLoPT, which is likely due to a larger increase of precipitation amounts. The three weather classes containing HiT are associated with a large increase of temperature and a moderate increase of rain and snowmelt with the exception of LoQHiT which shows a low increase of snowmelt (Figure 7). Lastly, MoQMoPT and LoQMoPT demonstrate similar change of precipitation and temperature, but MoQMoPT clearly has a higher increase in both rainfall and snowmelt compared to LoQMoPT. The main visual difference between watersheds was that a lower increase of snowmelt is expected in Big Creek

Hydrol. Earth Syst. Sci. Discuss., https://doi.org/10.5194/hess-2019-204
Manuscript under review for journal Hydrol. Earth Syst. Sci.
Discussion started: 21 May 2019

3.3 Atmospheric circulation and streamflow projections

The 50 members average change of temperature and precipitation between the historical period and the 2040's is shown in Figure 8. An increase of air temperature at 850hPa (T850) and geopotential height at 500hPa (Z500) is expected to occur within the entire domain with a stronger gradient closer to the Arctic (Figure 8c). precipitation is also simulated to increase by the 2040s throughout the domain while SLP is expected to decrease (Figure 8d). In the region close to the Great Lakes, the magnitude of warming and variability between members is higher on the northern shorelines as compared to the open water and shorelines south of the Lakes (Figure 8a). Precipitation increases is also projected to be higher on land and on the east side of the Great Lakes and toward the Atlantic coast (Figure 8b and 8d).

The internal contribution of each member of CanESM2-LE to the change of climate variables was averaged for each class (Figure 9). The class HiQHiPT is projected to be associated with positive temperature, precipitation, and southwesterly winds change anomalies between high pressure anomalies in the east and low pressure anomalies in west side of the domain (Figure 9a and 9h). LoQLoPT has opposite pressure gradient anomalies and is the only class that show negative increase of precipitation and temperature anomalies occurring simultaneously (Figure 9g and 9n). LoQMoPT demonstrates a similar pattern to LoQLoPT, but the negative pressure anomalies is attenuated, and precipitation increases is higher (Figure 9e and 9l). MoQHiT and LoQHiT are characterized by positive temperature and pressure change anomalies over southern Ontario, while MoQMoPT and MoQLoPT has an opposite pattern.

3.4 Antecedant conditions and streamflow

Alternative factors are examined that may help to explain the January-February evolution of streamflow between the historical and the future period. Figure 10 shows the change of precipitation amount in November-December, groundwater flow in January-February and amount of snowpack water equivalent for the first and the last day of the January-February period. November-December precipitation are expecting to increase for all classes but a large intraclass and interclass variability is shown. The classes HiHiPT, HiHiT, MoHiT and the two LoPT weather classes show visually a higher increase of November-December precipitation as compared to the other classes. The amount of snowpack water equivalent at the beginning of the January-February period is expected to decrease with low variability between the classes but a large intra-class variability (Figure 10). The snowpack at the end of January-February is expected to decrease significantly for all classes with a low intraclass variability. The groundwater flow shows visually a large difference between watersheds with a higher increase in Credit River and Grand River compared to Big Creek and Thames River.

Hydrol. Earth Syst. Sci. Discuss., https://doi.org/10.5194/hess-2019-204
Manuscript under review for journal Hydrol. Earth Syst. Sci.
Discussion started: 21 May 2019

4 Discussion

4.1 Historical simulations

The observed seasonal cycle of streamflow was visually well reproduced by the simulated CTL and ensemble data for the historical period (1961-1990) (Figure 3). However, the simulated streamflow from CTL and the ensemble overestimated streamflow between November and February in the Thames and Big Creek watersheds. The overestimation is stronger in January for the ensemble which can be attributed to an overestimation of precipitation (Figure 5). Winter overestimation were previously reported for the Grand River watershed (Erler et al., 2018) and was attributed to the representation of the winter processes and the monthly resolution. In our study the control simulations performed very well in Grand River suggesting that the hydrological model structure is not responsible for the discrepancies. The quality of CanGRD observations could be incriminated but CanGRD observations are very consistent between watersheds in January-February. However, precipitation amounts are higher in Big Creek and Thames River in December (Figure 5) and groundwater flows are not increasing as much as in the Grand River watershed in January-February (Figure 10). This result suggests a January-February overestimation of the simulated groundwater flow in the historical period to adjust to the excess of precipitation amount in December. This hypothesis is strengthened by the groundwater discharge parameter Gwflow_coef which is higher in Thames and Big Creek river (Table 2). These results highlight the cascade of uncertainties in hydrological modelling and the need of diversify the climate data and the number of watersheds that are used in the projections of streamflow.

4.2 Increase of streamflow amplified or attenuated by Z500 anomalies

Despite the discrepancies highlighted in the last section, the results show a clear increase of streamflow in January-February (Figure 3) which has been previously simulated for other watersheds in the Great Lakes region (Byun et al., 2019; Erler et al., 2018; Grillakis et al., 2011; Kuo et al., 2017). January-February streamflow increases are likely caused by temperature and precipitation increases (Figure 5 and 8) that causes rain and snowmelt amounts to rise (Figure 4). (Grillakis et al., 2011) used several hydrological models in a small catchment close to Lake Ontario and reported that streamflow increases are due to rainfall increases in January and snowmelt increases in February. In our study we found an increase of rain and snowmelt for both months (Figure 4). The future increase of January-February rain and snowmelt is due to a warming (Figure 8) that have a global feature (Hoegh-Guldberg et al., 2018). Warming amplitudes projected for southern Ontario with CanESM2-LE are conformed to the CMIP5 multi-model projections with the same RCP8.5 scenario (Zhang et al., 2019). January-February precipitation increases are likely to occur in a large part of the domain (Figure 8) which also conforms to other climate models (Zhang et al., 2019). Precipitation increase between Lake Ontario/Erie and the East coast (Figure 8) is not expected by the multi-model projections and is likely inherent to CanESM2-LE. This precipitation pattern is probably associated to stronger winds from the east coast (Atlantic Ocean) due to a higher pressure decrease on land (Figure 8).

The 50 members produce a variable increase of streamflow (Figure 3) which is likely due to the variability in atmospheric circulation (Figure 9). 14% of the ensemble shows a high increase of streamflow simultaneously with high geopotential height

anomalies near the Atlantic Ocean (Table 4 and Figure 9a and 9h). This geopotential height pattern has been previously found to be responsible for increased precipitation and temperature in the Great Lakes region (Mallakpour and Villarini, 2016; Thiombiano et al., 2017), thereby increasing the streamflow and high flow events (Bradbury et al., 2002; Mallakpour and Villarini, 2016). 14% of the ensemble corresponds to the opposite geopotential pattern attenuating streamflow increase due to a lowered warming and lowered precipitation (Table 4, Figure 7 and Figure 9g and 9n). 6% of the ensemble also shows a low warming but a moderate increase in precipitation and snowmelt (Figure 7 and 9f and 9m) which is likely due to the north-west wind anomalies that bring more snow into the region (Figure 9f and 9m). Another 16% of the ensemble shows a moderate increase in streamflow which may be driven by high-geopotential height anomalies on the Great Lakes (Figure 9b and 9i). This pattern drives moderate increases of snowmelt and the rain-to-snow ratio associated with strong warming (Figure 7, 9b and 9i). Correspondence between high geopotential height and high temperature on the Great Lakes in winter have been previously reported (Ning and Bradley, 2015).

4.3 Consistency in the weather classes

The weather classes that show high (HiPT), moderate (MoPT) and low (LoPT) warming and wetting trends or high warming-only trend (HiT) (Figure 7), are clearly linked to atmospheric circulation patterns (Figure 9). However, the classes shown in Figure 9 are composed of members that have their own atmospheric variability signatures. Z500 anomalies associated with each member were investigated to verify the consistency among the members of the same weather class (Figure 11).

The members that comprise classes HiPT show consistently high Z500 anomalies in the east coast (six out of eight members) (Figure 11). The remaining two members (#13 and #48) show higher Z500 anomalies north of the Great Lakes. Eight members of the class LoPT show low Z500 in the east coast but two members (#1 and #10) show low pressure in the northern side of the Great Lakes. HiT show generally high-pressure systems in the region of Great Lakes even though four of the thirteen members depict a different pattern (#2, #20, #31 and #47). Members in the MoPT class show low level pressure in the vicinity of the Great Lakes (Figure 9) but a high diversity in circulation patterns were observed (Figure 11). For the MoPT members, pressure gradients are generally lower (Figure 11) which indicates conditions closer to the global signal. This suggests there is greater impact of global or continental patterns on local weather conditions for the MoPT class members. Despite the differences between members of the same weather class, this study gives a good approximation of what to expect in term of the possible weather conditional changes and the associated regional atmospheric evolution.

4.4 Lag between atmospheric circulation shifts, local climate conditions and streamflow

Interclass variability in January-February streamflow increases is likely associated with temperature and precipitation variability. The weather class HiPT was found to be associated to high streamflow increases with MoQHiPT showing the lowest but still higher than average streamflow increase (Table 4). The weather class LoPT shows lower streamflow increase even though few members (class MoQLoPT) are associated with higher increase due to more precipitation and snowfall (Figure 7). However, within HiT and MoPT weather classes, the modulation of January-February weather conditions between the

historical period and 2040's translates to a large range of streamflow projections. Four of the thirteen HiT members and eight of the nineteen MoPT members demonstrate lower increases of streamflow (Table 4). These discrepancies between the evolution of weather conditions and streamflow are possibly due to the timing at which the change of temperature and precipitation occur. To account for the routing delay between the runoff and streamflow at the outlet, our analyses use a lag-time of 6 days between the precipitation/temperatures and the streamflow. Any remaining delay between weather conditions and streamflow could occur due to snow accumulation/melting and groundwater recharge/discharge. The differences between the MoPT classes and the HiT classes are very low in term of the starting snowpack volume (Figure 10) which suggests there is a low impact of late fall snowpack volume change on January-February streamflow change. However, the snowpack remaining at the end of January-February is decreasing at a higher rate for MoQMoPT class as compared to LoQMoPT (Figure 10) which may be associated with a higher increase in snowmelt (Figure 7). These two classes show very similar change of temperature and precipitation influence on streamflow (Figure 7) suggesting that weather conditions obscure intra-seasonal variability change. Indeed, a simultaneous or decoupled change in precipitation and temperature may differently impact the rain to snow ratio, the snowfall or the snowmelt. Variance within the HiT classes may be from similar processes. Despite similar change in temperature and precipitation, the decrease of remaining snowpack at the end of the period is weaker for LoQHiT compared to MoQHiT (Figure 10). The lower streamflow in LoQHiT may also be associated with a lower increase of groundwater flow due to a lower increase of November-December precipitation change (Figure 10). A further analysis shows a correlation between the 50 members November-December change of precipitations and the January-February change of groundwater flow close to 0.7 in each watershed. This correlation suggests an enhancement or attenuation of the streamflow in January-February due to the late-fall amount of precipitation. These results emphasize the implication of late fall atmospheric circulation for the evolution of winter streamflow. A late fall atmospheric circulation similar to HiT, favouring dry anomalies, will not have the same implication for winter streamflow compared to a pattern bringing rain. Similarly, an increase in snowfall, following by a cold period is expecting to delay the snowmelt and flow volume to early spring. The atmospheric patterns can also occur successively several times in the same month, which is expected to impact greatly the streamflow, especially high flows.

4.5 Spatial variability of streamflow change modulation

The changes in the amount of rain and snowmelt between the historical period and the 2040's are visually similar for three of the watersheds (Figure 7). The Big Creek watershed is distinctly different as it shows a lower snowmelt contribution to streamflow (Figure 7). This suggests that there will be less snow available to be melted in this watershed as it is situated in the southern part of the study area near Lake Erie and experiences the mildest winters (Figure 5). In this watershed, the snowmelt volume is expected to increase until the 2040s before decreasing during the second half of the 21th Century (Figure 3). The same trend is expected for Thames River because of its southerly latitude and lower elevation (Figure 3). In Grand River the snowmelt is expected to stabilize after the 2040s. In the Credit River watershed, the snowmelt may continue to increase after the 2040s. Additionally, the increase in snowmelt is expected to occur only in January for Thames River and Big Creek

watersheds while the increase will be stronger in February for Grand and Credit River. A similar South-North pattern is observed in previous studies. A high increase of streamflow in December and January followed by a decrease of streamflow in February was simulated for the Canard watershed near Lake Erie (Rahman et al., 2012) while this shift is expected to occur between February and March further north near Lake Ontario (Grillakis et al., 2011; Sultana and Coulibaly, 2011) or Lake Simcoe (Kuo et al., 2017; Oni et al., 2014). These results suggest that the peak in snowpack depletion will occur more and more early in the future, increasing strongly the winter streamflow in the first decades. Towards the end of the 21st century, the increase of streamflow will slow down due to the warming reducing the snowpack. This process will occur first in the warmest watersheds, classically situated further south, in low lands and close to the Great Lakes. However, similar to previous studies in southern Ontario, the reduced snowpack is not projected to decrease the streamflow in winter because the winter precipitation are also projected to increase as suggested in the majority of the climate models (Zhang et al., 2019).

5 Conclusion

This study used a 50-member ensemble of regional climate data, forced with the IPCC RCP8.5 scenario, as input in the PRMS hydrological model to show how the internal variability of climate is transferred to the near future winter (January-February) projections of streamflow in four diverse watersheds in southern Ontario. An ascending hierarchical classification was used to construct classes of similar change of temperatures/precipitations/streamflow and define streamflow change probabilities and associated regional atmospheric drivers. First, the results showed that all members of the ensemble are associated with a January-February increase in streamflow due to a strong warming trend and an increase in precipitation projected by the RCP8.5 scenario. Second, the results suggested that the future increase of temperature and precipitation in January-February will be modulated by the internal variability of climate with implication for hydrological processes. We projected:

(i) 14% of the ensemble showing a large (small) increase in the near future streamflow due to the modulation of rain and snowmelt associated with the development of high (low) pressure anomalies in the east coast of North America.
(ii) 16% of the ensemble showing a moderate streamflow enhancement due to an increase in the rainfall to snowfall ratio associated with warmer conditions driven by high pressure over the Great Lakes region.
(iii) 38% of the ensemble showing a change of temperature and precipitations close to the 50-members average with a small contribution of internal variability of climate to the long-term trends of temperature and precipitation in southern Ontario.

The evolution of streamflow in January-February will be also modulated by inter-member variability of groundwater recharge from November-December precipitation and by the evolution of snow accumulation/melting due to the timing of the increase of temperature and precipitation.

This study focussed on average change while the intra-seasonal variability of atmospheric circulation may greatly impact the streamflow and especial high-flows due to day to day variability. The use of the same regional ensemble together with a classification of daily atmospheric fields would be useful to assess the future projections of high-flows in the region. The results of this study are based on a single regional ensemble and are therefore subject to the internal characteristics of the global climate model. Future studies could use other global climate models and different scenarios and can be extended to the end of the 21st century. Other hydrological models could also be used to increase the confidence regarding the hydrological processes projections. This work is important to assess the natural variability of the hydrological projections and help the society to be prepared for large range of possible changes in flooding regimes in future.

Acknowledgments

Financial support for this study was provided by the Natural Sciences and Engineering Research Council (NSERC) of Canada through the FloodNet Project. We also acknowledge researchers at the Ouranos and Centre ESCER, Environment and Climate Change Canada and Natural Resources Canada for their contribution in providing climate data sets. Support from Global Water Future Program is also acknowledged.

References

Barnett, T. P., Adam, J. C. and Lettenmaier, D. P.: Potential impacts of a warming climate on water availability in snow-dominated regions, Nature, 438(7066), 303–309, doi:10.1038/nature04141, 2005.

Bliss, A., Hock, R. and Radić, V.: Global response of glacier runoff to twenty-first century climate change, J. Geophys. Res. Earth Surf., 119(4), 717–730, doi:10.1002/2013JF002931, 2014.

Boorman, D. B., Williams, R. J., Hutchins, M. G., Penning, E., Groot, S. and Icke, J.: A model selection protocol to support the use of models for water management, Hydrol. Earth Syst. Sci., 11(1), 634–646, 2007.

Bradbury, J. A., Dingman, S. L. and Keim, B. D.: New England drought and relations with large scale atmospheric circulation patterns, J. Am. Water Resour. Assoc., 38(5), 1287–1299, doi:10.1111/j.1752-1688.2002.tb04348.x, 2002.

Byun, K., Chiu, C.-M. and Hamlet, A. F.: Effects of 21st century climate change on seasonal flow regimes and hydrologic extremes over the Midwest and Great Lakes region of the US, Sci. Total Environ., 650, 1261–1277, doi:10.1016/j.scitotenv.2018.09.063, 2019.

Clark, M. P., Wilby, R. L., Gutmann, E. D., Vano, J. A., Gangopadhyay, S., Wood, A. W., Fowler, H. J., Prudhomme, C., Arnold, J. R. and Brekke, L. D.: Characterizing Uncertainty of the Hydrologic Impacts of Climate Change, Curr. Clim. Change Rep., 2(2), 55–64, doi:10.1007/s40641-016-0034-x, 2016.

Dai, A., Fyfe, J. C., Xie, S.-P. and Dai, X.: Decadal modulation of global surface temperature by internal climate variability, Nat. Clim. Change, 5(6), 555–559, doi:10.1038/nclimate2605, 2015.

Deser, C., Phillips, A. S., Alexander, M. A. and Smoliak, B. V.: Projecting North American climate over the next 50 years: uncertainty due to internal variability*, J. Clim., 27(6), 2271–2296, 2014.

Devia, G. K., Ganasri, B. P. and Dwarakish, G. S.: A Review on Hydrological Models, Aquat. Procedia, 4, 1001–1007, doi:10.1016/j.aqpro.2015.02.126, 2015.

Erler, A. R., Frey, S. K., Khader, O., d'Orgeville, M., Park, Y.-J., Hwang, H.-T., Lapen, D., Peltier, W. R. and Sudicky, E. A.: Simulating Climate Change Impacts on Surface Water Resources within a Lake Affected Region using Regional Climate Projections, Water Resour. Res., doi:10.1029/2018WR024381, 2018.

Fowler, H. J., Blenkinsop, S. and Tebaldi, C.: Linking climate change modelling to impacts studies: recent advances in downscaling techniques for hydrological modelling, Int. J. Climatol., 27(12), 1547–1578, doi:10.1002/joc.1556, 2007.

Gelfan, A., Semenov, V. A., Gusev, E., Motovilov, Y., Nasonova, O., Krylenko, I. and Kovalev, E.: Large-basin hydrological response to climate model outputs: uncertainty caused by internal atmospheric variability, Hydrol. Earth Syst. Sci., 19(6), 2737–2754, doi:10.5194/hess-19-2737-2015, 2015.

Grillakis, M. G., Koutroulis, A. G. and Tsanis, I. K.: Climate change impact on the hydrology of Spencer Creek watershed in Southern Ontario, Canada, J. Hydrol., 409(1–2), 1–19, doi:10.1016/j.jhydrol.2011.06.018, 2011.

Hamlet, A. F. and Lettenmaier, D. P.: Effects of 20th century warming and climate variability on flood risk in the western U.S., Water Resour. Res., 43(6), doi:10.1029/2006WR005099, 2007.

Harding, B. L., Wood, A. W. and Prairie, J. R.: The implications of climate change scenario selection for future streamflow projection in the Upper Colorado River Basin, Hydrol. Earth Syst. Sci., 16(11), 3989–4007, doi:10.5194/hess-16-3989-2012, 2012.

Hawkins, E. and Sutton, R.: The Potential to Narrow Uncertainty in Regional Climate Predictions, Bull. Am. Meteorol. Soc., 90(8), 1095–1108, doi:10.1175/2009BAMS2607.1, 2009.

Hoegh-Guldberg, O., Jacob, D., Taylor, M., Bindi, M., Brown, S., Camilloni, I., Diedhiou, A., Djalante, R., Ebi, K. L., Engelbrecht, F., Guiot, J., Hijioka, Y., Mehrotra, S., Seneviratne, S. I., Thomas, A., Warren, R., Halim, S. A., Achlatis, M., Alexander, L. V., Berry, P., Boyer, C., Byers, E., Brilli, L., Buckeridge, M., Cheung, W., Craig, M., Evans, J., Fischer, H., Fraedrich, K., Ganase, A., Gattuso, J. P., Bolaños, T. G., Hanasaki, N., Hayes, K., Hirsch, A., Jones, C., Jung, T., Kanninen, M., Krinner, G., Lawrence, D., Ley, D., Liverman, D., Mahowald, N., Meissner, K. J., Millar, R., Mintenbeck, K., Mix, A. C., Notz, D., Nurse, L., Okem, A., Olsson, L., Oppenheimer, M., Paz, S., Petersen, J., Petzold, J., Preuschmann, S., Rahman, M. F., Scheuffele, H., Schleussner, C.-F., Séférian, R., Sillmann, J., Singh, C., Slade, R., Stephenson, K., Stephenson, T., Tebboth, M., Tschakert, P., Vautard, R., Wehner, M., Weyer, N. M., Whyte, F., Yohe, G., Zhang, X., Zougmoré, R. B., Marengo, J. A., Pereira, J. and Sherstyukov, B.: Impacts of 1.5°C of Global Warming on Natural and Human Systems, , 138, 2018.

Ines, A. V. M. and Hansen, J. W.: Bias correction of daily GCM rainfall for crop simulation studies, Agric. For. Meteorol., 138(1–4), 44–53, doi:10.1016/j.agrformet.2006.03.009, 2006.

Kay, J. E., Deser, C., Phillips, A., Mai, A., Hannay, C., Strand, G., Arblaster, J. M., Bates, S. C., Danabasoglu, G., Edwards, J., Holland, M., Kushner, P., Lamarque, J.-F., Lawrence, D., Lindsay, K., Middleton, A., Munoz, E., Neale, R., Oleson, K., Polvani, L. and Vertenstein, M.: The Community Earth System Model (CESM) Large Ensemble Project: A Community Resource for Studying Climate Change in the Presence of Internal Climate Variability, Bull. Am. Meteorol. Soc., 96(8), 1333–1349, doi:10.1175/BAMS-D-13-00255.1, 2015.

Khakbaz, B., Imam, B., Hsu, K. and Sorooshian, S.: From lumped to distributed via semi-distributed: Calibration strategies for semi-distributed hydrologic models, J. Hydrol., 418–419, 61–77, doi:10.1016/j.jhydrol.2009.02.021, 2012.

Kour, R., Patel, N. and Krishna, A. P.: Climate and hydrological models to assess the impact of climate change on hydrological regime: a review, Arab. J. Geosci., 9(9), doi:10.1007/s12517-016-2561-0, 2016.

Kumar, S., Allan, R. P., Zwiers, F., Lawrence, D. M. and Dirmeyer, P. A.: Revisiting trends in wetness and dryness in the presence of internal climate variability and water limitations over land: WETNESS AND DRYNESS TRENDS OVER LAND, Geophys. Res. Lett., 42(24), 10,867-10,875, doi:10.1002/2015GL066858, 2015.

Kuo, C. C., Gan, T. Y. and Higuchi, K.: Evaluation of Future Streamflow Patterns in Lake Simcoe Subbasins Based on Ensembles of Statistical Downscaling, J. Hydrol. Eng., 22(9), 04017028, doi:10.1061/(ASCE)HE.1943-5584.0001548, 2017.

Lafaysse, M., Hingray, B., Mezghani, A., Gailhard, J. and Terray, L.: Internal variability and model uncertainty components in future hydrometeorological projections: The Alpine Durance basin, Water Resour. Res., 50(4), 3317–3341, doi:10.1002/2013WR014897, 2014.

Leduc, M., Mailhot, A., Frigon, A., Martel, J.-L., Ludwig, R., Brietzke, G. B., Giguère, M., Brissette, F., Turcotte, R., Braun, M. and Scinocca, J.: The ClimEx Project: A 50-Member Ensemble of Climate Change Projections at 12-km Resolution over Europe and Northeastern North America with the Canadian Regional Climate Model (CRCM5), J. Appl. Meteorol. Climatol., 58(4), 663–693, doi:10.1175/JAMC-D-18-0021.1, 2019.

Leng, G., Huang, M., Voisin, N., Zhang, X., Asrar, G. R. and Leung, L. R.: Emergence of new hydrologic regimes of surface water resources in the conterminous United States under future warming, Environ. Res. Lett., 11(11), 114003, doi:10.1088/1748-9326/11/11/114003, 2016.

Lorenz, E. N.: Deterministic Nonperiodic Flow, J. Atmospheric Sci., 20(2), 130–141, doi:10.1175/1520-0469(1963)020<0130:DNF>2.0.CO;2, 1963.

Mallakpour, I. and Villarini, G.: Investigating the relationship between the frequency of flooding over the central United States and large-scale climate, Adv. Water Resour., 92, 159–171, doi:10.1016/j.advwatres.2016.04.008, 2016.

Markstrom, S. L., Regan, R. S., Hay, L. E., Viger, R. J., Payn, R. A. and LaFontaine, J. H.: precipitation-runoff modeling system, version 4: U.S. Geological Survey Techniques and Methods., 2015.

McKenney, D. W., Hutchinson, M. F., Papadopol, P., Lawrence, K., Pedlar, J., Campbell, K., Milewska, E., Hopkinson, R. F., Price, D. and Owen, T.: Customized Spatial Climate Models for North America, Bull. Am. Meteorol. Soc., 92(12), 1611–1622, doi:10.1175/2011BAMS3132.1, 2011.

Moriasi, D. N., Arnold, J. G., Van Liew, M. W., Bingner, R. L., Harmel, R. D. and Veith, T. L.: Model evaluation guidelines for systematic quantification of accuracy in watershed simulations, Trans. ASABE, 50(3), 885–900, 2007.

Ning, L. and Bradley, R. S.: Winter climate extremes over the northeastern United States and southeastern Canada and teleconnections with large-scale modes of climate variability*, J. Clim., 28(6), 2475–2493, 2015.

Oni, S. K., Futter, M. N., Molot, L. A., Dillon, P. J. and Crossman, J.: Uncertainty assessments and hydrological implications of climate change in two adjacent agricultural catchments of a rapidly urbanizing watershed, Sci. Total Environ., 473–474, 326–337, doi:10.1016/j.scitotenv.2013.12.032, 2014.

Rahman, M., Bolisetti, T. and Balachandar, R.: Hydrologic modelling to assess the climate change impacts in a Southern Ontario watershed, Can. J. Civ. Eng., 39(1), 91–103, doi:10.1139/l11-112, 2012.

Rowell, D. P.: Sources of uncertainty in future changes in local precipitation, Clim. Dyn., 39(7–8), 1929–1950, doi:10.1007/s00382-011-1210-2, 2012.

Schoof, J. T.: Statistical Downscaling in Climatology: Statistical Downscaling, Geogr. Compass, 7(4), 249–265, doi:10.1111/gec3.12036, 2013.

Seiller, G. and Anctil, F.: Climate change impacts on the hydrologic regime of a Canadian river: comparing uncertainties arising from climate natural variability and lumped hydrological model structures, Hydrol. Earth Syst. Sci., 18(6), 2033–2047, doi:10.5194/hess-18-2033-2014, 2014.

Stephens, G. L., L'Ecuyer, T., Forbes, R., Gettelmen, A., Golaz, J.-C., Bodas-Salcedo, A., Suzuki, K., Gabriel, P. and Haynes, J.: Dreary state of precipitation in global models: MODEL AND OBSERVED PRECIPITATION, J. Geophys. Res. Atmospheres, 115(D24), doi:10.1029/2010JD014532, 2010.

Sultana, Z. and Coulibaly, P.: Distributed modelling of future changes in hydrological processes of Spencer Creek watershed, Hydrol. Process., 25(8), 1254–1270, doi:10.1002/hyp.7891, 2011.

Thiombiano, A. N., El Adlouni, S., St-Hilaire, A., Ouarda, T. B. M. J. and El-Jabi, N.: Nonstationary frequency analysis of extreme daily precipitation amounts in Southeastern Canada using a peaks-over-threshold approach, Theor. Appl. Climatol., 129(1–2), 413–426, doi:10.1007/s00704-016-1789-7, 2017.

Thompson, D. W. J., Barnes, E. A., Deser, C., Foust, W. E. and Phillips, A. S.: Quantifying the Role of Internal Climate Variability in Future Climate Trends, J. Clim., 28(16), 6443–6456, doi:10.1175/JCLI-D-14-00830.1, 2015.

Wu, W.-Y., Lan, C.-W., Lo, M.-H., Reager, J. T. and Famiglietti, J. S.: Increases in the annual range of soil water storage at northern middle and high latitudes under global warming, Geophys. Res. Lett., 42, 3903–3910, doi:10.1002/2015gl064110, 2015.

Zhang, Flato, G., Wan, H., Wang, X., Rong, R., Fyfe, J., Li, G., Kharin, V.V., Kirchmeier-Young, M, Vincent, L, Wan, H., Wang, X, Rong, R., Fyfe, J., Li, G. and Kharin, V.V.: Canada's Changing Climate Report, Government of Canada, Ottawa, Ontario., 2019.

Zhuan, M.-J., Chen, J., Shen, M.-X., Xu, C.-Y., Chen, H. and Xiong, L.-H.: Timing of human-induced climate change emergence from internal climate variability for hydrological impact studies, Hydrol. Res., 49(2), 421–437, doi:10.2166/nh.2018.059, 2018.

Hydrol. Earth Syst. Sci. Discuss., https://doi.org/10.5194/hess-2019-204
Manuscript under review for journal Hydrol. Earth Syst. Sci.
Discussion started: 21 May 2019

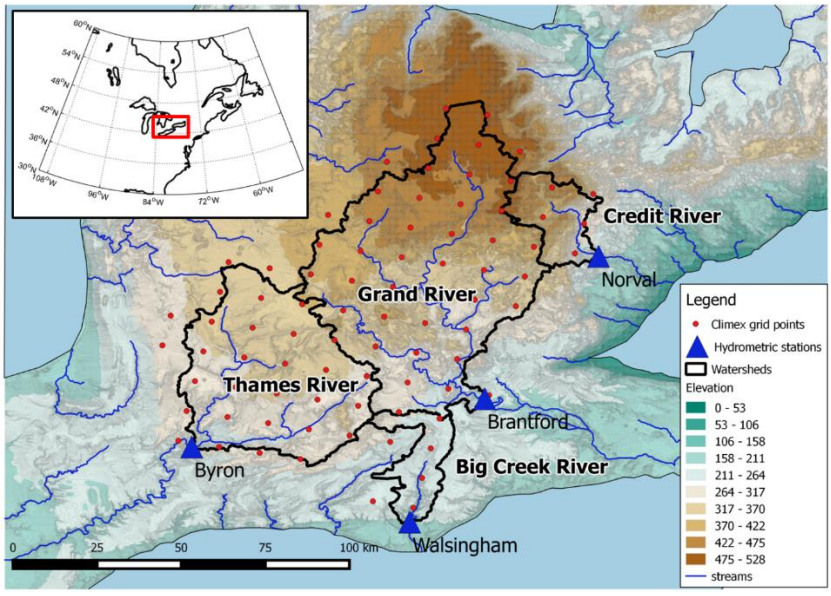

Figure 1: Location map of the four studied watersheds in Southern Ontario.

5

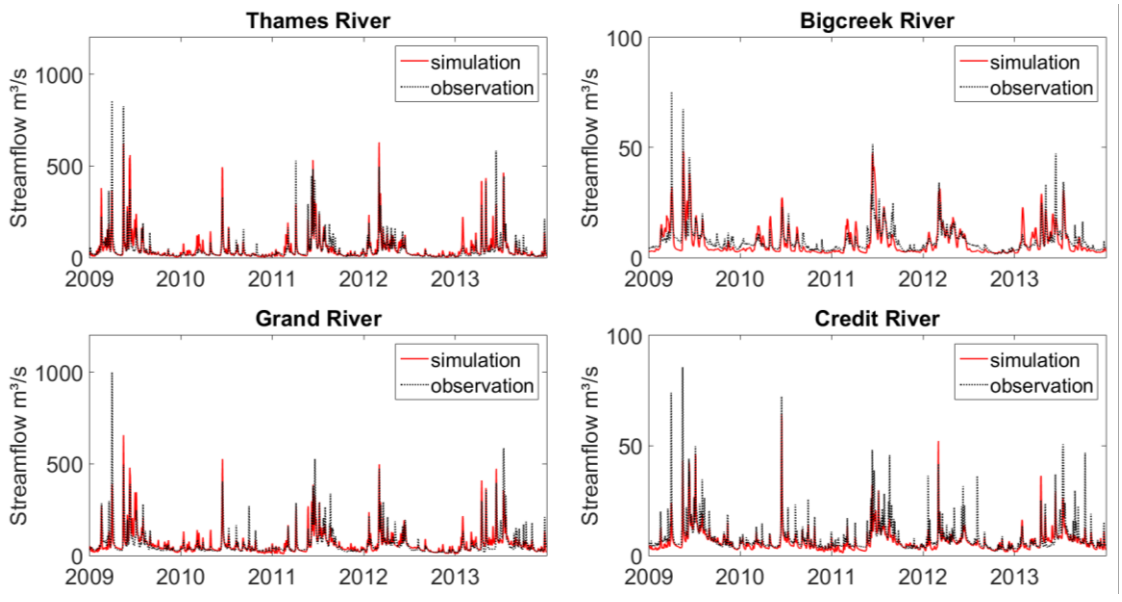

Figure 2: Daily observed (OBS) and simulated (CTL) streamflow during the validation period (2009-2013).

Hydrol. Earth Syst. Sci. Discuss., https://doi.org/10.5194/hess-2019-204
Manuscript under review for journal Hydrol. Earth Syst. Sci.
Discussion started: 21 May 2019

Hydrology and Earth System Sciences
Discussions
Open Access
EGU

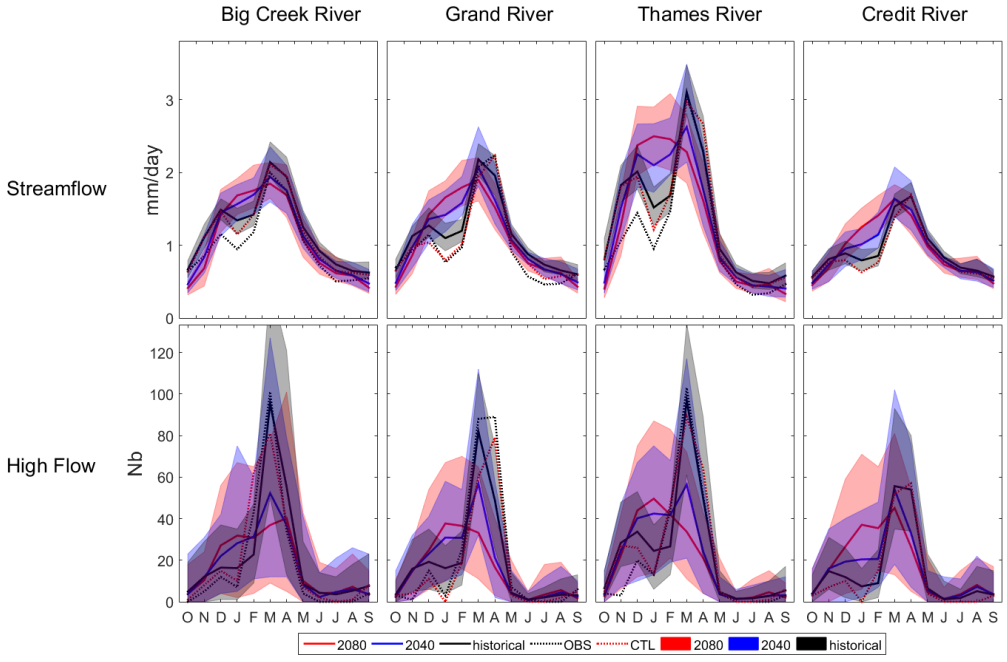

Figure 3: 50-members range and average streamflow and number of high-flows for the historical and two future periods.

Hydrol. Earth Syst. Sci. Discuss., https://doi.org/10.5194/hess-2019-204
Manuscript under review for journal Hydrol. Earth Syst. Sci.
Discussion started: 21 May 2019

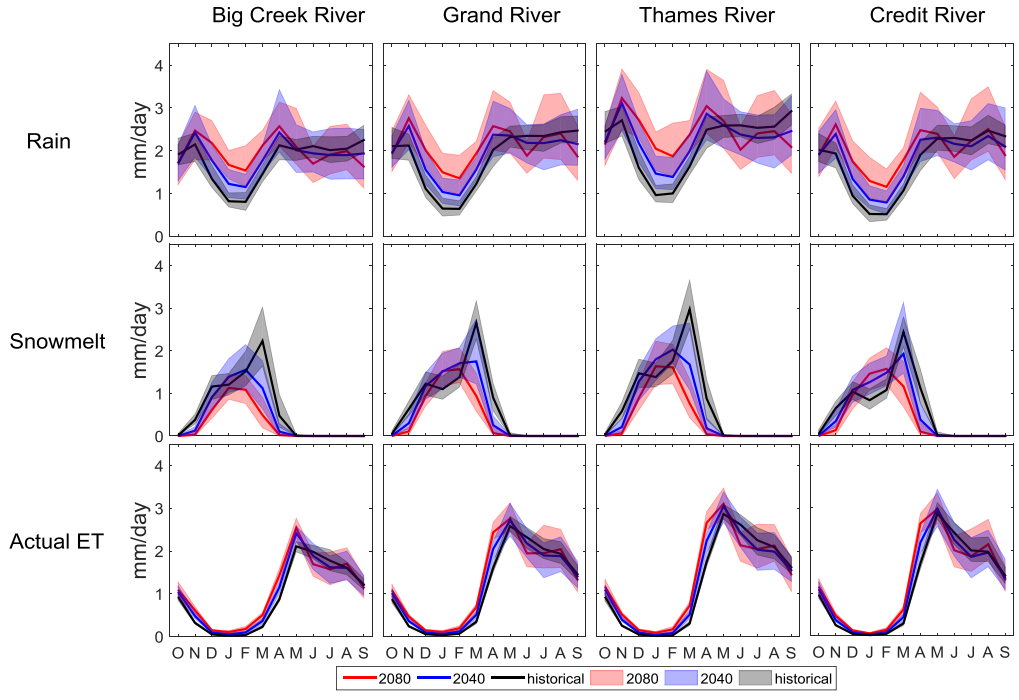

Figure 4: 50-members range and average rain, snowmelt and actual ET amounts for the historical and two future periods.

Hydrol. Earth Syst. Sci. Discuss., https://doi.org/10.5194/hess-2019-204
Manuscript under review for journal Hydrol. Earth Syst. Sci.
Discussion started: 21 May 2019

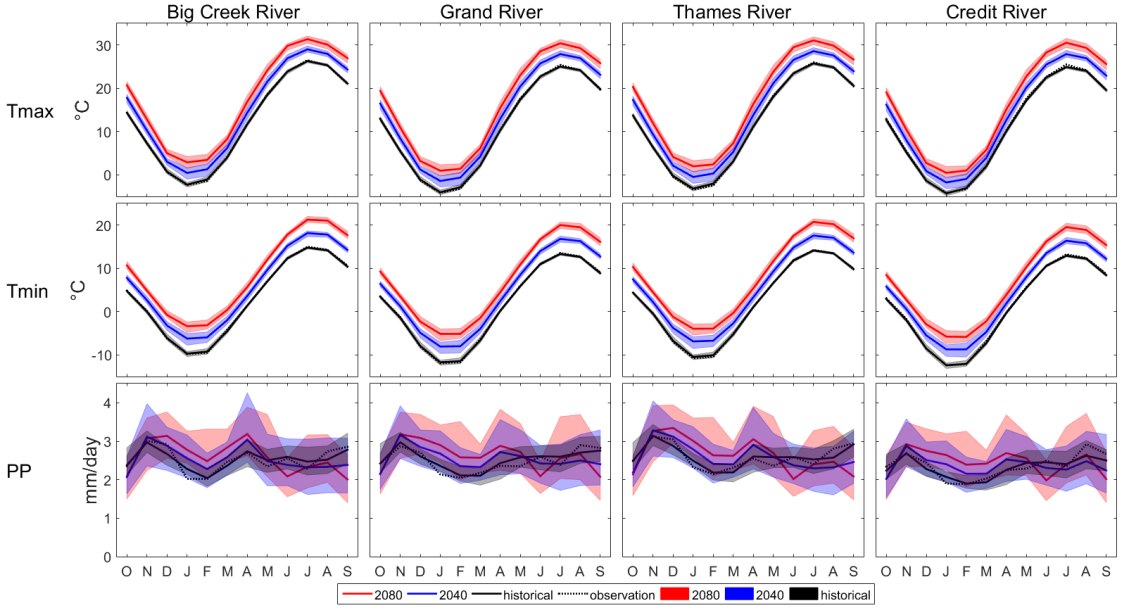

Figure 5: 50-members range and average temperature and precipitation amounts for the historical and two future periods.

Hydrol. Earth Syst. Sci. Discuss., https://doi.org/10.5194/hess-2019-204
Manuscript under review for journal Hydrol. Earth Syst. Sci.
Discussion started: 21 May 2019

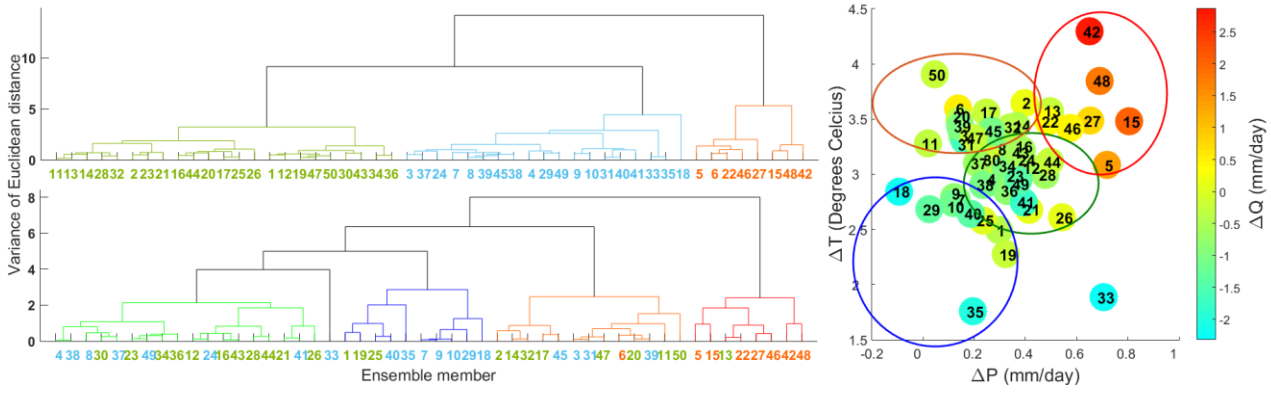

Figure 6 Left: Results of the Ascending Hierarchical Classification (AHC) for the normalized change of streamflow (Q) (above) and normalized change of average Temperature (T) and Precipitation (P) (below). Colored numbers represent Q classes. Right: 4-watersheds average change of streamflow (Q) (Colors) with respect to average change of P and T. Large hollow circles represent the 4 weather classes.

Hydrol. Earth Syst. Sci. Discuss., https://doi.org/10.5194/hess-2019-204
Manuscript under review for journal Hydrol. Earth Syst. Sci.
Discussion started: 21 May 2019

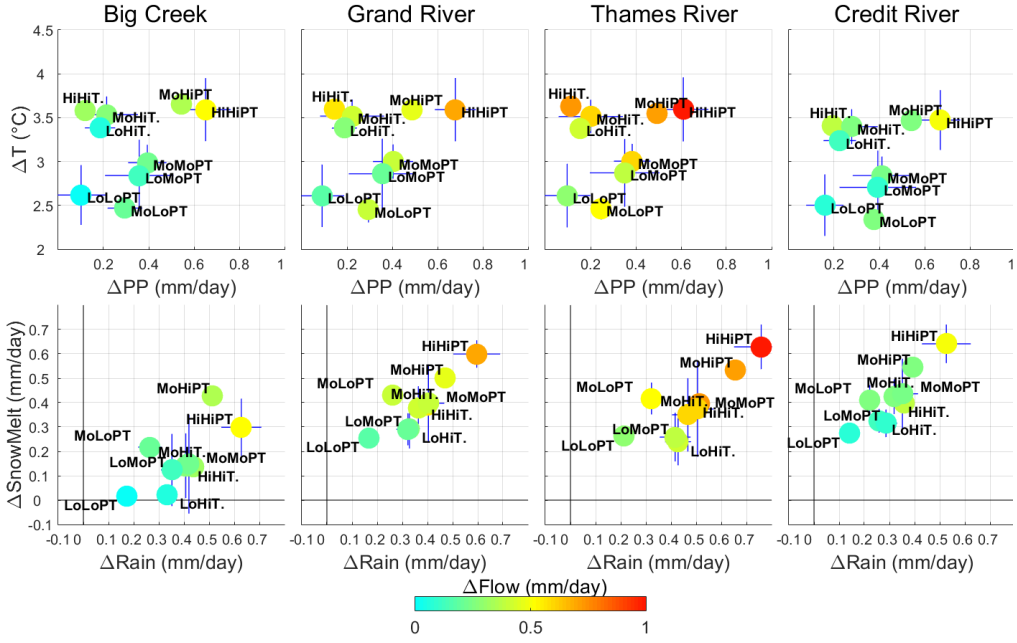

Figure 7: Change of streamflow (Colors) with respect to changes of daily temperature and precipitation amount (above) and snowmelt and rain amounts (Below) between the historical and the 2040's future period in January-February.

Hydrol. Earth Syst. Sci. Discuss., https://doi.org/10.5194/hess-2019-204
Manuscript under review for journal Hydrol. Earth Syst. Sci.
Discussion started: 21 May 2019

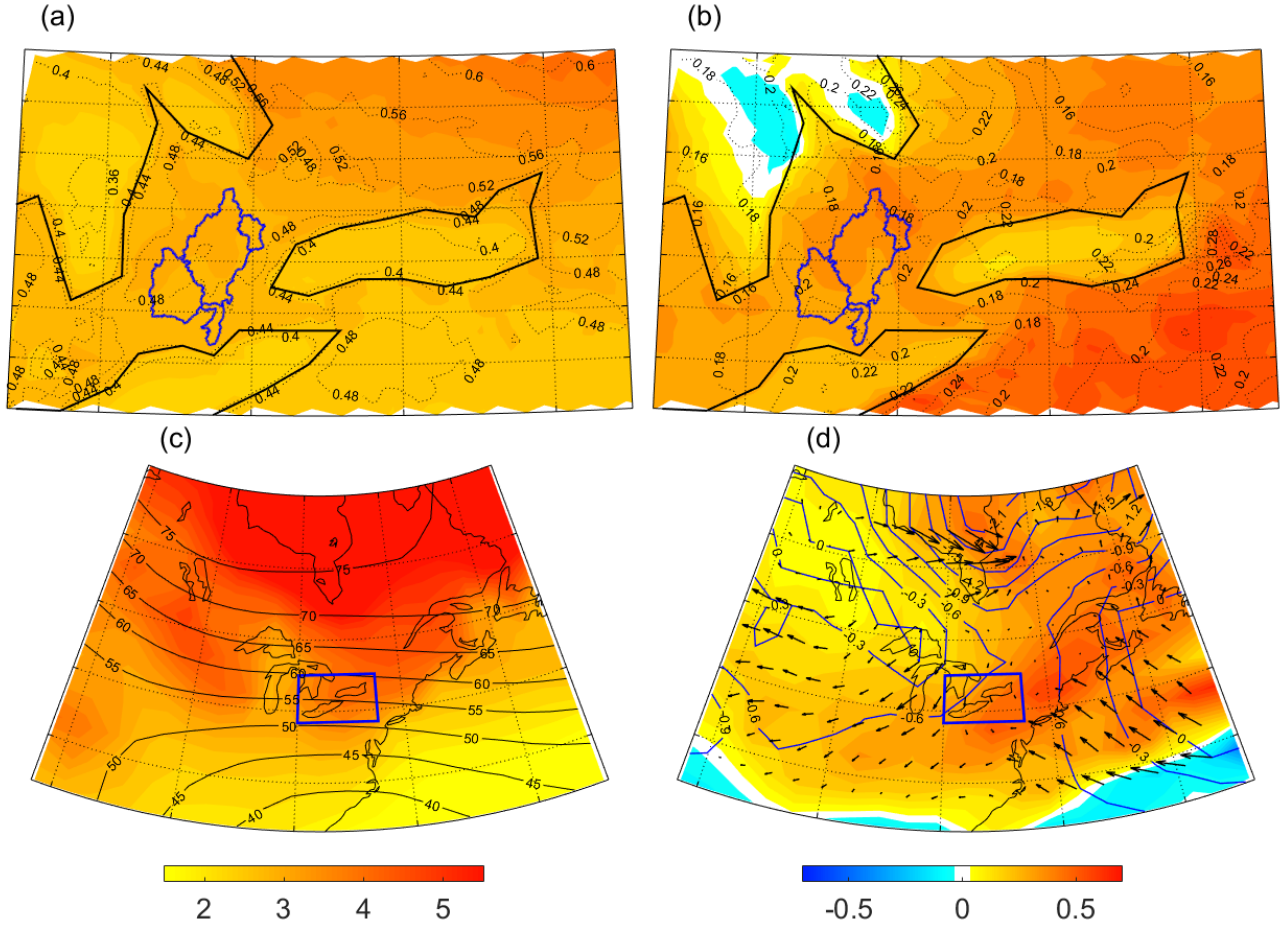

Figure 8. 50-members ensemble average change of atmospheric conditions between the historical and the 2040's period in January-february for a. CRCM5-LE average temperature (shade) and standard deviation (black lines), b. CRCM5-LE average precipitation (shade) and standard deviation (black lines), c. CanESM2-LE T850 (shade) and Z500 (black lines) and d. CanESM2-LE precipitation (shade), SLP (blue lines) and wind (vectors).

Hydrol. Earth Syst. Sci. Discuss., https://doi.org/10.5194/hess-2019-204
Manuscript under review for journal Hydrol. Earth Syst. Sci.
Discussion started: 21 May 2019

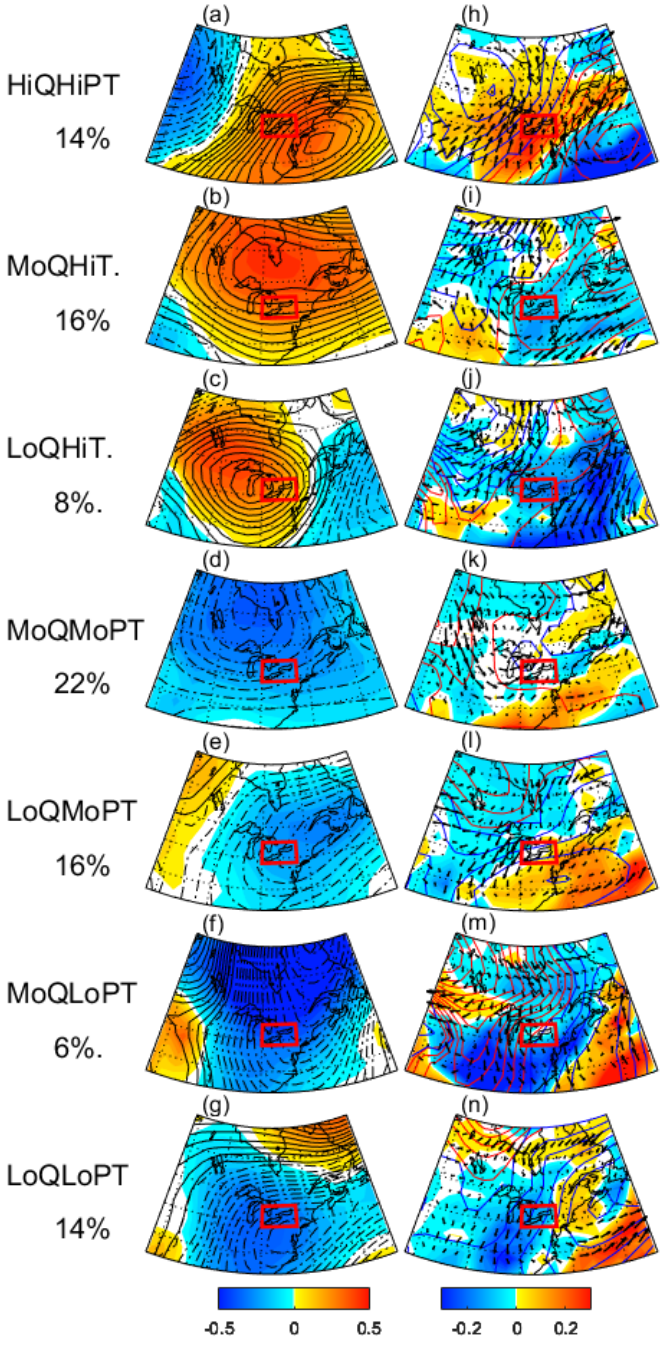

Figure 9: a-g: Classes averaged internal contribution of a-g T850 (shade) and Z500 (black lines, in intervals of 1m) and h-n: Precipitations (shade), SLP (lines, in intervals of 0.1Pa) and wind (vectors) to the 50-members average change between the historical and the 2040's period in January-February.

Hydrol. Earth Syst. Sci. Discuss., https://doi.org/10.5194/hess-2019-204
Manuscript under review for journal Hydrol. Earth Syst. Sci.
Discussion started: 21 May 2019

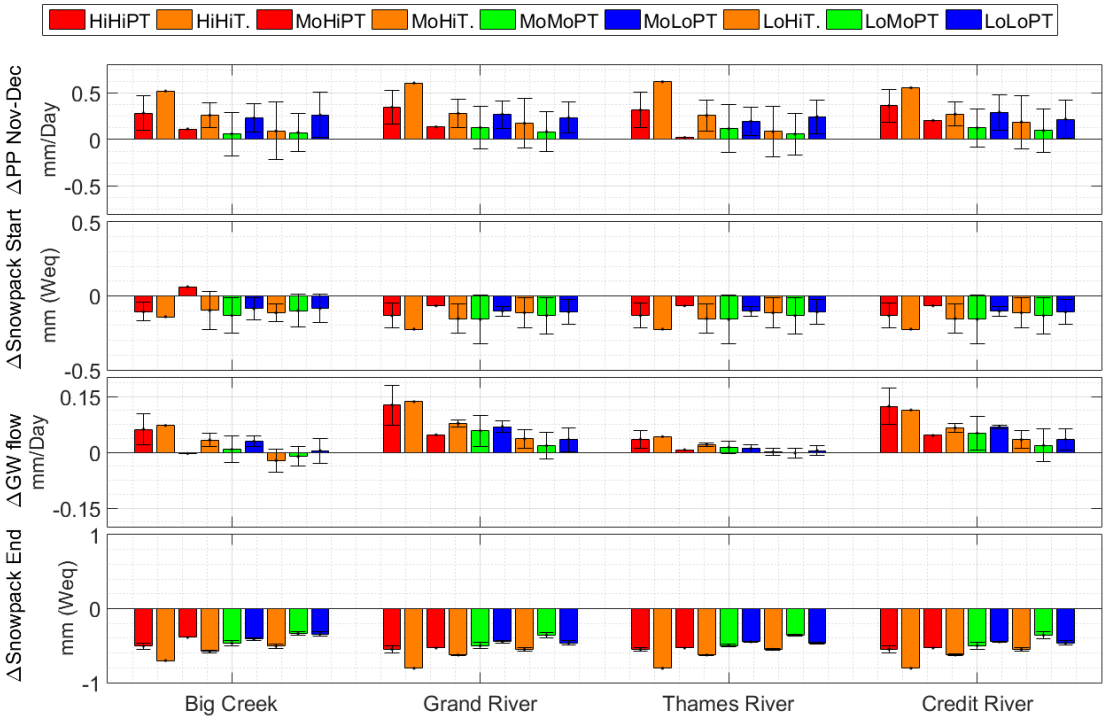

Figure 10: Evolution between the historical and 2040's period for first row: precipitation amount (mm) in November-December, second row: snowpack amount (mm water-equivalent) in December 25th, third row: Groundwater flow in January-February and fourth row: snowpack amount (mm water-equivalent) in February 23th.

Hydrol. Earth Syst. Sci. Discuss., https://doi.org/10.5194/hess-2019-204
Manuscript under review for journal Hydrol. Earth Syst. Sci.
Discussion started: 21 May 2019

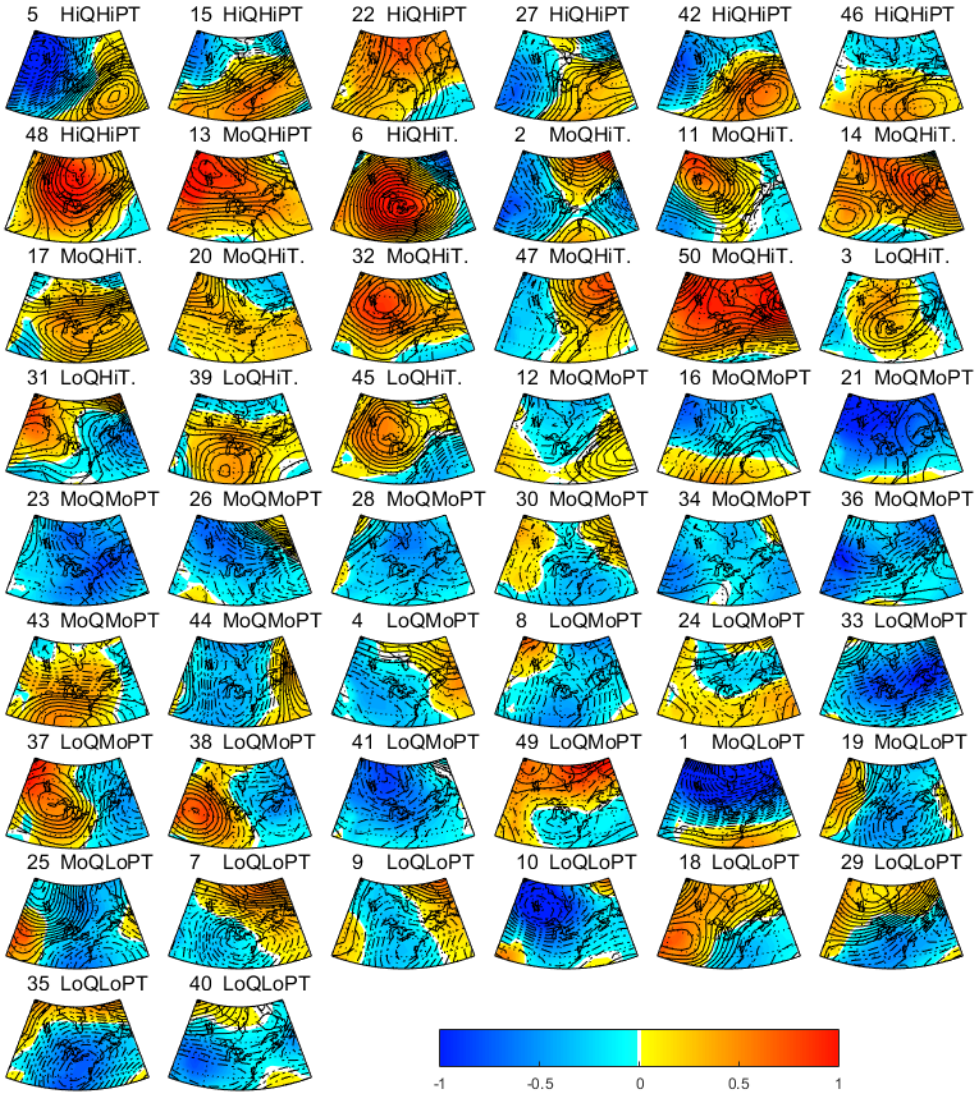

Figure 11: Internal change of T850 (shade) and Z500 (black lines, interval 2m) between the historical and the 2040's period in January-February for each member.

Hydrol. Earth Syst. Sci. Discuss., https://doi.org/10.5194/hess-2019-204
Manuscript under review for journal Hydrol. Earth Syst. Sci.
Discussion started: 21 May 2019

Hydrology and Earth System Sciences
Discussions

Table 1: Geomorphic, land use, and soil characteristics of the four watersheds examined in this study

	Size (km²)	Altitude (m)	Land use (%)				Soil type (%)		
			Barren	Forest	Shrub	Crops/Grass	Sand	Loam	Clay
Big Creek	571	179-336	1.9	17	0	81.1	78.6	6.4	15
Grand River	5091	178-531	7.1	11.9	0	80.9	30.4	31.6	38
Thames River	3061	215-423	6.9	5.4	0	87.7	14	46.7	39.4
Credit River	646	190-521	6.6	31.7	0	61.8	42.5	49.1	8.4

Hydrol. Earth Syst. Sci. Discuss., https://doi.org/10.5194/hess-2019-204
Manuscript under review for journal Hydrol. Earth Syst. Sci.
Discussion started: 21 May 2019

Hydrology and Earth System Sciences
Discussions

Table 2 Parameter values after calibration (C= Calibrated, GIS= estimated by arcpy_GSFLOW)

Parameter	Unit	Big Creek	Grand River	Thames River	Credit River	Spatial and temporal	Source
dday_intcp	Degrees days	-27 – -10	-26 – -9	-26 – -11	-26 – -9	monthly	C
dday_slope	Degrees days / °F	0.38 – 0.41	0.38 – 0.42	0.38 – 0.42	0.38 – 0.42	monthly	C
tmax_index	°F	29.3 – 80	31.2 – 78	29.3 – 80	26.5 – 78.3	monthly	C
jh_coef	per °F	0.005 – 0.021	0.005 – 0.02	0.005 – 0.021	0.003 – 0.02	monthly	C
Jh_coef_hru	per °F	22 – 22.9	20.4 – 21.4	20.7 – 21.3	20.4 – 21.5	HRU	GIS
Adjmix_rain	Decimal fraction	0	0	1	0	One	C
Cecn_coef	Calories per °C > 0	20	15	10	0	One	C
emis_noppt	Decimal fraction	0.757	0.757	0.757	0.757	One	C
Fastcoef_lin	Fraction / day	0.001	0.2	0.1	0.2	One	C
Fastcoef_sq	none	0.005	0.1	0.4	0.5	One	C
Freeh2o_cap	inches	0.07	0.01	0.01	0.01	One	C
Gwflow_coef	Fraction / day	0.01	0.05	0.06	0.03	One	C
Potet_sublim	Decimal fraction	0.1	0.75	0.1	0.6	One	C
Smidx_coef	Decimal fraction	0.0001	0.05	0.04	0.001	One	C
Smidx_exp	1 / inch	0.2	0.2	0.2	0.3	One	C
Soil_rechr_max	inches	0.24 – 1.81	0.24 – 1.84	0.2 – 1.9	0.71– 5.5	HRU	GIS+C
Soil_moist_max	inches	1.2 – 9.1	0.79 – 6.12	0.8 – 6.3	0.79 – 6.1	HRU	GIS
Tmax_allrain	°F	34	35	33	36	One	C
hru_percent_ imperv	Decimal fraction	0.1 – 0.6	0.1 – 0.6	0.1 – 0.6	0.1 – 0.6	HRU	GIS
Carea_max	Decimal fraction	0.4 – 0.9	0.4 – 0.9	0.4 – 0.9	0.4 – 0.9	HRU	GIS
Ssr2gw_exp	none	3	1	1.5	3	One	C
Ssr2gw_rate	Fraction / day	0.30 – 0.95	0.02 – 0.66	0.01 – 0.26	0.02 – 0.47	HRU	GIS+C
Slowcoef_sq	none	0.0004 – 7.6	0 – 133	0.002 – 1.97	0 – 11.9	HRU	GIS+C
Slowcoef_lin	Fraction / day	0.02 – 12.3	0 – 0.07	0.004 –0.71	0 – 0.33	HRU	GIS+C
K_coef	hours	2.8 – 8.4	1.6 – 3.2	1.78 – 3.56	1.35 – 2.68	Segment	GIS+C
Pref_flow_den	Decimal Fraction	0.1	0.1	0.1	0.2	One	C

Rain_adj	Decimal Fraction	0.77 – 0.86	0.69 – 1.12	0.92 – 1.04	0.87 – 0.94	HRU Monthly	GIS
Snow_adj	Decimal Fraction	0.96 – 1.06	0.69 – 1.12	0.92 – 1.04	0.72 – 0.76	HRU Monthly	GIS

Hydrol. Earth Syst. Sci. Discuss., https://doi.org/10.5194/hess-2019-204
Manuscript under review for journal Hydrol. Earth Syst. Sci.
Discussion started: 21 May 2019

Hydrology and Earth System Sciences
Discussions

Table 3: Efficiency of PRMS model for best fit parameters

	Calibration		Validation	
	NSE	PBIAS	NSE	PBIAS
Big Creek	0.75	1.8	0.74	6.7
Grand River	0.71	-5	0.69	1.7
Thames River	0.72	-10.8	0.72	-5.3
Credit River	0.71	-0.1	0.65	18

Hydrol. Earth Syst. Sci. Discuss., https://doi.org/10.5194/hess-2019-204
Manuscript under review for journal Hydrol. Earth Syst. Sci.
Discussion started: 21 May 2019

Hydrology and Earth System Sciences
Discussions

Table 4: Classes members, percentage of the total member in the class and average January-February increase of streamflow between historical and 2040's period.

Name	Members	%	ΔQ (mm/day)			
			Big Creek	Grand River	Thames River	Credit River
HiQHiPT	5,15,22,27, 42,46,48	14%	0.43 (0.09)	0.55 (0.10)	0.73 (0.11)	0.43 (0.09)
HiQHiT	6	2%	0.32	0.46	0.57	0.35
MoQHiPT	13	2%	0.33	0.40	0.56	0.29
MoQHiT	2,11,14,17, 20,32,47,50	16%	0.29 (0.05)	0.37 (0.03)	0.49 (0.08)	0.27 (0.02)
MoQMoPT	12,16,21,23,26,28, 30,34,36,43,46	22%	0.25 (0.05)	0.36 (0.04)	0.49 (0.06)	0.26 (0.04)
MoQLoPT	1,19,25	6%	0.25 (0.02)	0.36 (0.02)	0.44 (0.02)	0.28 (0.02)
LoQHiT	3,31,39,45	8%	0.15 (0.03)	0.29 (0.02)	0.38 (0.02)	0.19 (0.04)
LoQMoPT	4,8,24,33, 37, 38,41,49	16%	0.19 (0.06)	0.25 (0.04)	0.36 (0.05)	0.17 (0.06)
LoQLoPT	7,9,10,18, 29,35,40	14%	0.12 (0.11)	0.23 (0.06)	0.30 (0.10)	0.16 (0.05)